Two-component fluorescent semiconducting hydrogel from NDI-appended peptide with long chain amines: Variation of thermal and mechanical strength of gels

Nibedita Nandi,[†] Shibaji Basak,[†] Steven Kirkham,[#] Ian W. Hamley[#] and Arindam Banerjee*[,†]

[†]Department of Biological Chemistry, Indian Association for the Cultivation of Science, Jadavpur, Kolkata, 700032 (India) Fax: (+ 91) 33-2473-2805, E-mail: bcab@iacs.res.in.

[#]Department of Chemistry, University of Reading, Whitenights, Reading, RG6, 6AD, UK.

ABSTRACT

Two-component fluorescent hydrogels have been discovered containing mixtures of naphthalenediimide (NDI)-conjugated peptide-functionalized bola-amphiphile and primary amines with long alkyl chains at physiological pH 7.46. The aggregation induced enhanced emission (AIEE) associated with NDI-appended peptide in aqueous medium is rare, as water is known to be a good quencher of fluorescence. In this study, NDI-containing gelator peptide forms a highly fluorescent aggregate in aqueous medium. Absorption and emission spectroscopic techniques reveal the formation of J-aggregates among the chromophoric moieties in their aggregated state in aqueous medium. However, this NDI-containing peptide doesn't form any gel in aqueous medium. In presence of primary amines with long alkyl chains in buffer solution, it forms two-component fluorescent hydrogels exhibiting a bright yellow fluorescence under the UV-lamp (365 nm). Probably, the acid-amine interaction between the amines and the bola-amphiphile triggers the gel formation, as it is evident from Fourier transformed infrared (FTIR) data

indicating the presence of carboxylate group (-COO^-) and ammonium species (NH_3^+) in the co-assembled two-component gel system. Low and wide angle powder X-ray diffraction (PXRD), small angle X-ray scattering (SAXS) further supports the fact that the co-assembled state in the gel form is produced by the supramolecular interaction between the NDI-based bola-amphiphile and the long chain amines. Field emission scanning electron microscopy (FE-SEM) and high resolution transmission electron microscopy (HR-TEM) images reveal that the π-conjugated co-assembled hydrogels exhibit nano-fibrillar network morphologies. Interestingly, the co-assembled hydrogels exhibit an enhanced fluorescence emission, excited state lifetime and quantum yield compared to those of the NDI-containing amphiphile alone in its self-assembled state in aqueous medium. Moreover, thermal stability and mechanical strength of these gels have been successfully tuned by varying the alkyl chain length of the corresponding amine. Moreover, these NDI-peptide conjugated soft-materials exhibit semiconducting behavior in their respective co-assembled states. This holds future promise to use these peptide appended NDI-based co-assembled soft materials for the application in opto-electronic and other devices.

INTRODUCTION

Supramolecular soft materials[1-10] have become a rapidly expanding area in current research for the last few years. Among these soft materials, low molecular weight hydrogelators (LMWHG)[11-16] are currently finding potential applications in drug delivery, tissue engineering, bio-sensing and other related fields.[17-26] Most of these gels are obtained from a single component gelator molecule in aqueous medium. There are several examples of two component gels[27-29] that provide better diversity and tunability compared to that of single component gels. In these cases, the gelation property as well as thermal and mechanical properties can also be easily controlled by changing the molar ratio of these two components or by varying one of these two components. This offers great promise to design and construct new supramolecular soft materials with structural diversity and tunable functional properties.

Over the past two decades, significant efforts have been devoted to understand the structure-function relationship of organic π-conjugated n-type semiconducting material building blocks due to their various applications in organic electronic devices including photovoltaics, field-effect transistors as well as in fluorescent bio-probes.[30-38] Among several π-conjugated organic building blocks, molecular planarity, high π-acidity and the characteristic photo-physical behavior made NDIs an important candidate compared to the higher analogue of rylene dyes in supramolecular research.[39-42] Recently, NDI-peptide conjugates have proven advantageous to make new functional supramolecular soft materials with interesting applications because of their ability to self-assemble by using various non-covalent interactions including π-π interactions, van der Waals' interactions, hydrogen bonding interactions and others.[43-45] Because of very weakly fluorescent behavior, NDIs have limited capacity to exhibit good optical properties in their monomeric states.[46] However, supramolecular assembly of the NDI-based system has been studied with great interest because of their interesting photo-physical characteristics like J-aggregation, excimer emission, aggregation induced enhanced emission (AIEE) and others. AIEE is an effect of the particular assembly of the NDI-based system and the aggregated species (generally the J-aggregate) exhibits enhanced emission compared to the molecules in their respective monomeric states.[47-51] However, these organic π-conjugated molecules (rylene dyes) generally show non-fluorescent behavior in water due to the aggregation caused quenching (ACQ) phenomenon.[52] Due to reduction of photoluminescence efficiency and intrinsic hydrophobicity of the aromatic core, the optical study of the NDI-derivatives in aqueous environment has been limited.[43] Several previous studies have been directed to explore the assembly of NDI-derivatives in aqueous medium[53,54] and there are only a few reports on the assembly of NDI/peptide conjugated soft-materials[55,56] in aqueous medium. Parquette and co-workers have reported the formation of NDI-dilysine peptide based self-supporting hydrogel.[57] There are a few reports on the formation of NDI-based hydrogels under physiological conditions and the hydrogelation of NDI/amino-acid conjugates.[58-60] However, none of these examples include the self-assembly of NDI-appended peptide that not only form two-component hydrogels with long chain amines, but also promotes aggregation induced fluorescence in aqueous medium. To the best of our knowledge, this is the first

example of NDI-appended peptide based two-component hydrogel (with long chain alkyl amines) that shows aggregation induced fluorescence in aqueous medium. The merit of this two-component system is to tune the thermal, mechanical and photo-physical properties of the assembled NDI-system by varying chain length of the alkyl amine. Interestingly, fluorescence properties (fluorescence intensity, quantum yield, fluorescence lifetime in excited state) of this NDI-based moiety are remarkably changed in two-component gel system compared to that of the self-assembly of NDI-based peptide alone in water. Encouraged by the intriguing photo-physical properties of NDI-moieties we are curious to study the effect of self-assembly of the chromophoric moiety on the electrical conductance of NDI-based functional soft-materials.

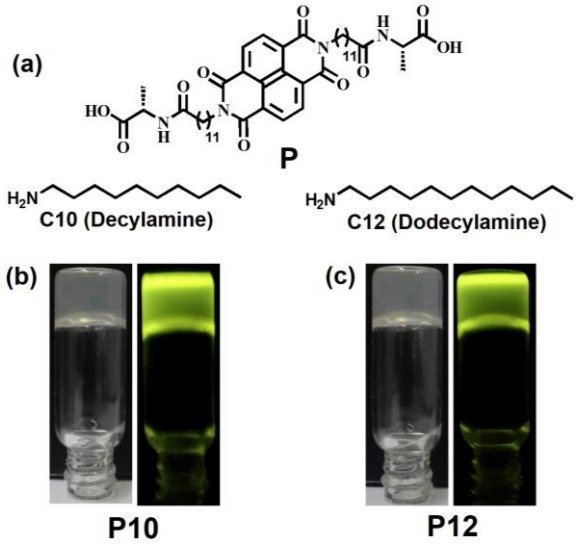

Figure 1. (a) Chemical structures of the peptide (**P**) and amines decylamine (C10) and dodecylamine (C12). (b) and (c) Photographs of two-component hydrogels **P10** (**P** with C10) and **P12** (**P** with C12) at a 1:2 molar ratio of peptide: amine in daylight (left side) and under UV lamp (right side) (365 nm) respectively.

In this study, utilizing a rational design, we report an unprecedented two-component fluorescent hydrogel system based on an NDI-conjugated dipeptide functionalized bola-amphiphile **P** and long chain primary alkyl amines in physiological phosphate buffer solution at pH 7.46 (Figure 1). The NDI-based bola-amphiphile has been chosen in such a way that it can be self-associated utilizing π-π interactions involving the NDI core, hydrogen bonding interactions using the intervening amide (-CONH) moieties, van der Waals' interactions from the intervening poly-methylene units of the NDI-based peptide as well

as from the long fatty acyl chain, and electrostatic interactions between the carboxylate ($-COO^-$) group and ammonium ($-NH_3^+$) species of the long chain amine. This newly formed hydrogel is fluorescent and emits a bright greenish-yellow color on illumination under UV lamp (365 nm).

EXPERIMENTAL SECTION

L-Alanine (L-Ala), 12-aminododecanoic acid (DNDA) and 1,4,5,8-Naphthalenetetracarboxylic dianhydride (NDA) were purchased from Aldrich. Decylamine (C_{10}), Dodecylamine (C_{12}), 1-hydroxybenzotriazole (HOBt), N, N'-dicyclohexylcarbodiimide (DCC) and all solvents were purchased from SRL, India**.** Details of the synthetic procedures of gelator peptide, instrumentation details, and spectroscopic analysis are given in the Supporting Information.

RESULTS AND DISCUSSION

Gelation Study

The NDI-based peptide **P** did not form gel by itself in phosphate buffer solution of pH 7.46, however, in the combination of both the peptide **P** and one of these long chain amines (C10 or C12) provided a two-component hydrogel. The gel is stable in the pH range 7.0 to 8.5 and it is also thermo-reversible in nature. The gelation propensities of this two-component system were studied in buffer solution by dissolving the peptide **P** with each amine by changing their proportions. The stable molar ratio of the peptide **P** and amines was found to be 1:2. Interestingly, any co-assembly with molar ratio of peptide **P**: amine = 1:1 did not form stable hydrogels in the buffer solution (pH 7.46), but a viscous solution was appeared (Figure S1). Only when the molar ratio was increased to 1:2, transparent hydrogel was obtained (Figure 1). For the other combinations like peptide **P**: amine = 1:3 and 1:4, the systems were

also unable to form any gel in the buffer solution of pH 7.46 (Figure S1). The gelation ability of the peptide P was examined using different primary long chain amines such as n-octylamine, n-decylamine, n-dodecylamine and n-tetradecyl amine. It is worth noting that the gelation was occurred only for decylamine and dodecylamine. However, the other two long chain amines failed to form such gel under the same conditions. The mixture of peptide **P** with n-octylamine formed a soluble aggregate, while the mixture obtained from tetra-decylamine was very hard to dissolve and gave a precipitate under the same conditions. This fact shows that the gel formation is dependent on the chain length of the corresponding alkyl amine. The gelation properties for the two-component systems were also studied with different amines including secondary amines, tertiary amines, cyclic amines, aromatic amines; but the gelation occurred only with long chain aliphatic primary amines. In this paper, a detailed study of the gel properties for decylamine containing two-component aggregate (**P10** hydrogel) (Figure 1b) and dodecylamine containing two-component aggregate (**P12** hydrogel) (Figure 1c) are included at 1: 2 ratio of peptide **P** and corresponding amine. Minimum gelation concentration (MGC) values were found to be 0.07 % (w/v) for the gel **P10** and 0.04 % (w/v) for the gel **P12**. The MGC values were calculated with respect to the peptide **P**. The gel melting temperatures (T_{gel}) of these hydrogels were found to be 40 ^{0}C and 47 ^{0}C for the gels **P10** and **P12** respectively at 1.25 mM concentration. This indicates the modulation of thermal stability by the variation of the alkyl chain length of the corresponding amine in two-component hydrogels (Table S1). This type of trend was also previously observed in two-component dendritic organogels.[28]

Morphological Study

To obtain a clear overview of the morphological features of the two-component hydrogel system, high resolution transmission electron microscopy (HR-TEM) and field emission scanning electron microscopy (FE-SEM) experiments were carried out. The HR-TEM images (Figure 2a and b) and FE-SEM images (Figure 2c and d) of the xerogels (obtained from hydrogels **P10** and **P12** at pH 7.46) show the nano-fibrillar morphologies for both of these hydrogels. These images reveal that these aggregates are

composed of numerous nano-fibers that are elongated to several micrometers in length. These nano-fibres are entangled with each other in a long range to form a nano-fibrillar gel network structure that entraps the water molecules to form a self-supported gel. Careful inspection of FE-SEM image reveals that the nano-fibres are 50-60 nm in width and twisted in nature, although some of them are bundled up to form fibers with relatively more thickness. The different strategies to sample preparation for FE-SEM and HR-TEM studies may be the reason for the difference in appearance of these fibers in different morphological studies.

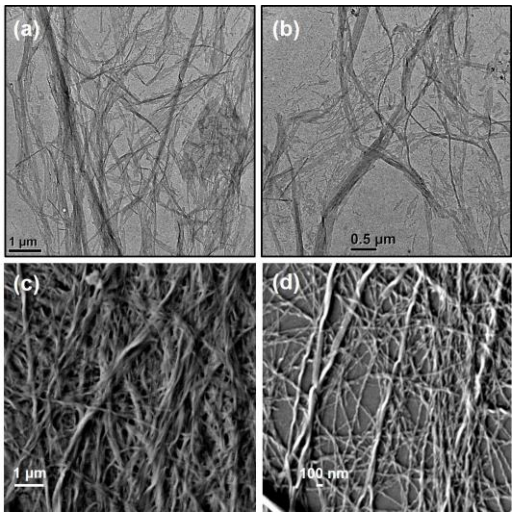

Figure 2. (a), (b) HR-TEM and (c), (d) FE-SEM images of the xerogels obtained from **P10** and **P12** hydrogels (at a 1:2 molar ratio of peptide: amine) respectively.

Rheological Study

To obtain fundamental mechanical properties and flow behavior of the two-component hydrogels, rheological experiments have been carried out at a constant oscillatory frequency of 1 Hz at room temperature (25 ^{o}C). In a frequency sweep rheological experiment presented in Figure 3, it is observed that the storage modulus (G') values are higher than the loss modulus (G") values for both hydrogels **P10** and **P12** (at 1:2 molar ratio of peptide: amine) at 2.5mM concentration. In these experiments, G' and G" did not cross each other (G' > G") and they are found to be almost parallel to the angular frequency applied throughout the experimental region. These observations suggest soft ‘solid-like’ gel phase formation. It is evident from the plot that the co-assembled hydrogel **P12** with longer alkyl chain amine

has a 6-fold increase in G' and G" values compared to those of **P10** hydrogel with relatively shorter alkyl chain amine. The longer aliphatic chain of C12 probably allows the assembly of the bola-amphiphile **P** with C12 in a more sterically favorable conformation than C10 and this makes **P12** hydrogel more robust than **P10** hydrogel.[28] Rheological studies were performed in other two concentrations (2 mM and 3 mM) to explore the possibility of variance of storage and loss moduli of these co-assembled gels **P10** and **P12** (Figure S5). It was found that both storage and loss moduli of these two gels were dependent on the concentration.

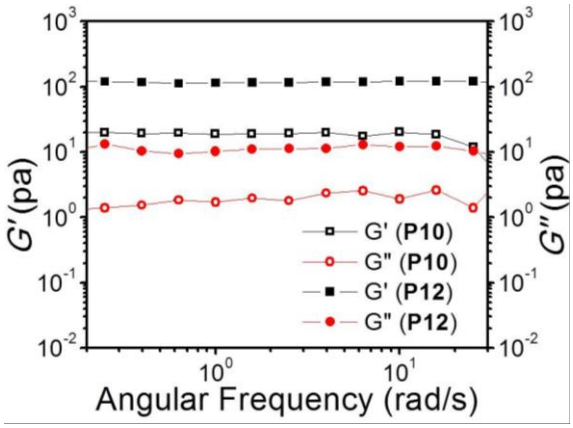

Figure 3. Log–log plot of storage modulus (G') and loss modulus (G") versus angular frequency of the hydrogels **P10** and **P12** (at a 1:2 molar ratio of peptide: amine) at 2.5 mM concentration.

Time-Correlated Single-Photon-Counting (TCSPC) Study

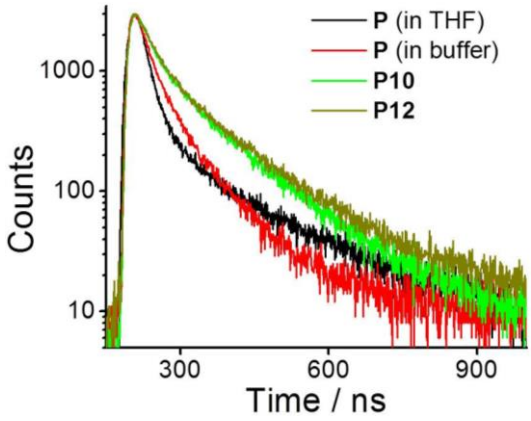

Figure 4. TCSPC decay profiles obtained from peptide **P** (in THF and buffer solution), two-component aggregates **P10** and **P12** (at a 1:2 molar ratio of peptide: amine) at 0.05mM concentration.

Time-correlated single-photon-counting (TCSPC) experiments were performed to get insights into the aggregation induced change in emission properties of the peptide **P**. In THF, the excitation monochromator was set to 340 nm and the emission was recorded at 410 nm for peptide **P**. Short-lived decay was noticed with an average lifetime 721 ps, arising for the monomeric NDI fluorophore due to the fast intersystem crossing to close-lying triplet state. Similar experiments were performed for peptide **P** in aqueous medium (buffer solution of pH 7.46) with an excitation at 340 nm and the emission was monitored at 527nm. At 527 nm, a tri-exponential decay was observed with a substantially longer average lifetime of 1.99 ns (Figure 4). The concentration of peptide **P** was kept constant at 0.05 mM throughout the experiment. For the experiments conducted using co-assembled aggregated system **P10** and **P12**, on excitation at 340 nm the emissions were recorded at 529 nm and 531 nm respectively. In these cases, the resultant decay profiles also show a tri-exponential decay with a substantially longer average lifetime of 3.18 ns and 3.33 ns respectively. These observations also suggest that the excited state complexes of **P10** and **P12** are significantly more stable than that the peptide **P** alone in aqueous medium. Notably, the quantum yield of the peptide **P** was found to be 3.6% in aqueous medium using quinine sulphate as a reference dye. However, the quantum yields for the two-component aggregated systems **P10** and **P12** were found as 4.2% and 5.4% respectively using the same reference dye (quinine suphate). The detailed data for TCSPC study and quantum yield are tabulated in Table 1. These observations may be due to the fact that the aggregation of the co-assembled system is more profound in two-component aggregated system than the aggregation of the self-assembled NDI-based peptide **P** alone in aqueous medium. Moreover, the co-assembled aggregate **P12** with comparatively long alkyl chain amine induces the assembly of the NDI-fluorophore more than the aggregate **P10** with an amine with shorter alkyl chain length.

Table 1. Quantum Yield (Φ) and fluorescence lifetime in excited state (with time component τ_1, τ_2, τ_3) obtained from TCSPC measurements of peptide **P** (in THF and buffer solution) and for two-component aggregates **P10** and **P12** (at a 1:2 molar ratio of peptide: amine).

Sample	Quantum Yield Φ (%)	τ_1(%) ns	τ_2(%) ns	τ_3(%) ns	Average lifetime τ_{avg} (%) ns
Peptide **P** (in THF)	-	0.046 (99.0)	0.011 (0.8)	0.015 (0.2)	0.072
Peptide **P** (in water)	3.6	0.910 (73.5)	0.936 (25.2)	0.149 (1.31)	1.99
P10	4.2	0.961 (23.2)	1.295 (15.5)	0.922 (61.3)	3.18
P12	5.4	1.036 (66.9)	1.703 (28.5)	0.596 (4.6)	3.33

Spectroscopic Study

To get an overview about the aggregation pattern of the two-component co-assembled system, a photo-physical study was performed in the self-associated state of peptide **P**. For this purpose, UV-vis spectroscopic study of the peptide **P** was performed to examine the aggregation pattern from monomeric chromophore to the aggregated state by changing the solvent from THF to buffer solution (pH 7.46) and then by systematically increasing the amine concentration in the system. The concentration of peptide **P** was kept constant at 0.005 mM throughout the experiment. In Figure 5 the peptide **P** shows well-resolved sharp absorption bands in the range of 300–400 nm in THF. This arises due to a π-π* transition along the long axis of the chromophore in the monomeric state. In THF, peaks appeared at 379 nm and 359 nm with a shoulder around 340 nm. However, when the solvent system was changed from THF to buffer solution, the peptide **P** tends to form aggregates in aqueous medium. This is evident from the bathochromic shift (11 nm) and about a 60 % decrease of the lowest energy absorption peak (379 nm) as shown in Figure 5. For the two-component complex **P10** (at 1:2 molar ratio of **P** and C12), a similar type of change in peak position was observed, that shows a bathochromic shift of 11 nm and a 59% decrease of absorbance for the lowest energy peak was observed (Figure 5a). However, the peak position for **P12** aggregate was slightly different from **P10** aggregate. For **P12** aggregate (at 1:2 molar ratio of **P** and C12), there was a 6

nm red shift and a 68% decrease in absorbance upon aggregation (Figure 5b). However, at 1: 1 molar ratio of peptide **P** and C12, a 8 nm red shift and a 64% decrease of absorbance of the lowest energy peak was observed. The red shift and remarkable decrease in the lowest energy absorption peak in all aqueous medium suggest that the J-aggregated π-π stacking is present in the aggregated state of the chromophore.[42,43] The concentration dependent UV-vis spectroscopy were performed at 1:2 molar ratio of peptide: amine for both **P10** and **P12** aggregated system (Figure S6) at 0.005 mM concentration of peptide **P**. The peaks appeared at similar position (389 nm) and the absorption was observed with a regular increase with increase in concentration of the peptide **P** (inset figure 5).

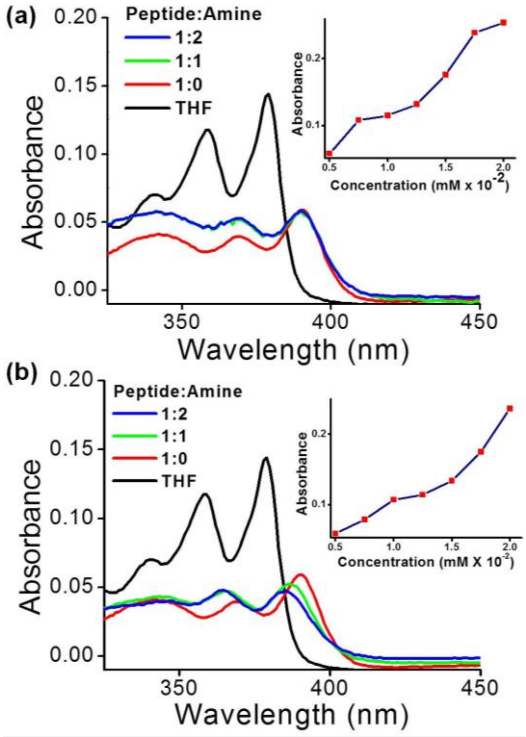

Figure 5. (a) Absorption spectra obtained from monomeric (in THF) and aggregated (in buffer solution) states of peptide **P** and two-component **P10** aggregates (at 1:1 and 1:2 molar ratios of peptide: amine). (b) Absorption spectra obtained from monomeric (in THF) and aggregated (in buffer solution) states of peptide **P** and two-component **P12** aggregates (at 1:1 and 1:2 molar ratios of peptide: amine). Inset of figures: Absorbance at 389 nm with increasing concentration of **P10** and **P12** aggregates respectively at a 1:2 molar ratio of peptide: amine. The concentration of peptide **P** was 0.005 mM for all these cases.

To get more insight about the optical property of the two-component co-assembled system, a photoluminescence (PL) study was done for the peptide **P** in both THF and buffer solution (pH 7.46) at

0.5 mM concentration. The solvent change from THF to buffer solution can significantly alter the aggregation pattern followed by a drastic change in fluorescence behavior. In THF, a very small emission band was observed at 410 nm due to the non-aggregated state of the chromophore at an excitation of 340 nm. It exhibits a very weak emission in THF, but emits a strong greenish-yellow fluorescence with more than a 300-fold increase in emissive intensity upon aggregation in the buffer solution (pH 7.46). For this case, the emission spectra showed two prominent bands centered at 460 nm and 550 nm as apparent in Figure 6a and b. An intense peak around 527 nm accompanied by a broad emission band around 435-460 nm suggests the aggregation induced enhancement of emission (AIEE) of NDI-based peptide **P** in aqueous medium. After the addition of C10 to make a 1:1 proportional mixture with peptide **P**, the peak intensity around 529 nm was gradually increased (Figure 6a). At 1: 2 molar ratio of **P** and C10, this peak intensity was further increased. The PL spectrum for this two-component aggregate **P12** is quite different from that of **P10** aggregate. At 1: 1 molar ratio of **P** and C12, an enhancement of the peak intensity was noticed around 430 nm accompanied by a broad peak around 529 nm (Figure 6b). The intensity of these peaks gradually increased while changing the molar ratio from 1:1 to 1:2. In addition to that, a broad emission band around 530-560 nm was also noticed for **P12** aggregate at 1:2 molar ratio of peptide **P**: amine. Therefore, the two-component co-assembled systems **P10** and **P12** emits greenish-yellow colored fluorescence under the UV lamp (365 nm).

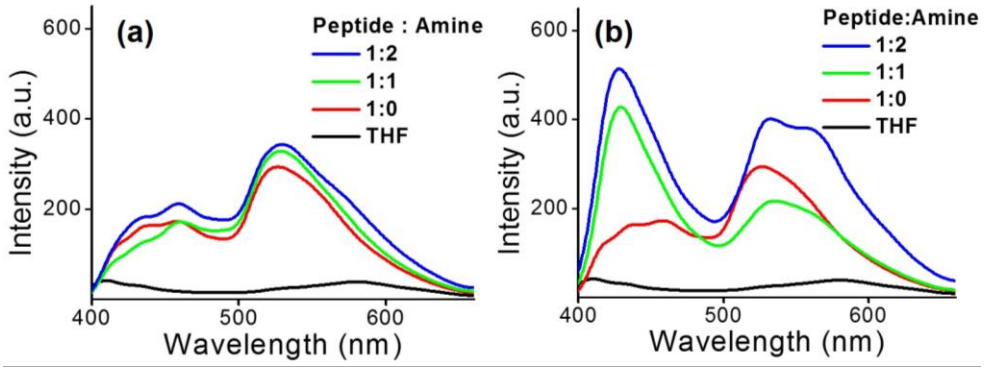

Figure 6. (a) Emission spectra obtained from monomeric (in THF) and aggregated (in buffer solution) states of peptide **P** and two-component **P10** aggregates (at 1:1 and 1:2 molar ratios of peptide: amine) upon excitation at 340 nm. (b) Emission spectra obtained from monomeric (in THF) and aggregated (in buffer solution) states of peptide **P**

and two-component **P12** aggregates (at 1:1 and 1:2 molar ratios of peptide: amine) upon excitation at 340 nm. The concentration of peptide **P** was 0.5 mM for all these cases.

Powder X-ray Diffraction (PXRD) and Small Angle X-ray Scattering (SAXS) Studies

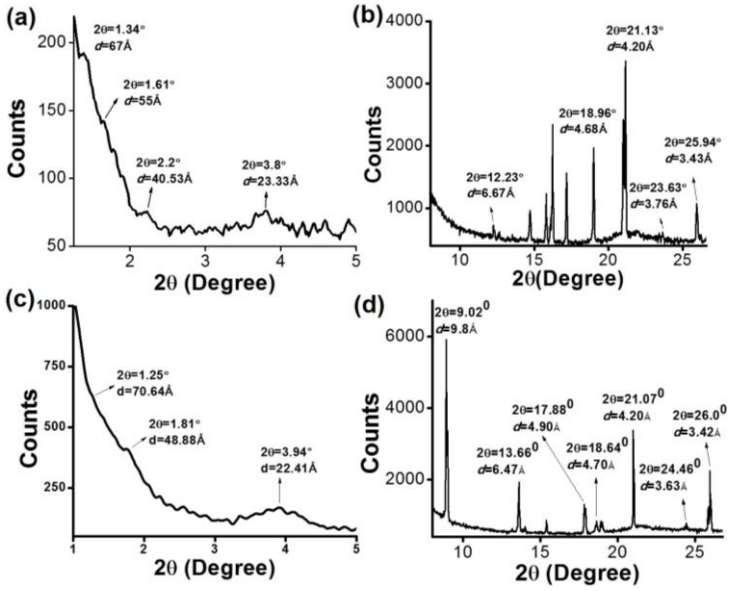

Figure 7. (a), (c) Low angle PXRD and (b), (d) Wide angle PXRD pattern obtained from the xerogels of **P10** and **P12** hydrogels (at a 1:2 molar ratio of peptide: amine) respectively.

The internal packing arrangement of the self-assembled hydrogel was investigated by both wide angle and low angle powder X-ray diffraction (PXRD) for the xerogels obtained from **P10** and **P12** hydrogels at the molar ratio 1:2 of peptide **P** and amine. In the low angle region (Figure 7a and b), distinct peaks at $2\theta=2.2^0$ (d= 40.53Å) and $2\theta=1.81^0$ (d= 48.88Å) were observed for **P10** and **P12** respectively. These values matched well with the calculated molecular length (44.28 Å) of peptide **P** on its own. In the SAXS data for **P12** hydrogel, a peak appeared corresponding to a d value 43.47Å, also in good agreement with the length of the molecule **P** (Figure S7). A broad peak corresponding to a d-spacing value of 67Å ($2\theta=1.34^0$) and 70.64Å ($2\theta=1.25^0$) were observed for **P10** and **P12** respectively from low angle PXRD and for both cases these values are close to the calculated total length of the peptide **P** (74.84Å) with two amines (C10 and C12) in the assembled structure as depicted in a tentative model in Figure 8. The reflection peaks appeared at $2\theta=3.8^0$ (d= 23.33Å) and $2\theta=3.94^0$ (d= 22.41Å) for **P10** and **P12** respectively correspond to second order peaks from a structure with a spacing equal to the molecular length of **P**. In

the wide angle region (Figure 7c and d), peaks are observed at $2\theta=9.02^0$ and $2\theta=18.64^0$ correspond to the *d*-spacing value of 9.8Å and 4.7Å respectively for **P12** indicating a sheet-like assembly in the gel state.[61] A peak at $2\theta=25.94^0$ with a *d*-spacing value 3.43Å was observed for **P10**, which is the characteristic peak for the π-π stacking of NDI core. Similar characteristic peak also appeared at $2\theta=26.0^0$ with corresponding *d* value of 3.42 Å for **P12**.

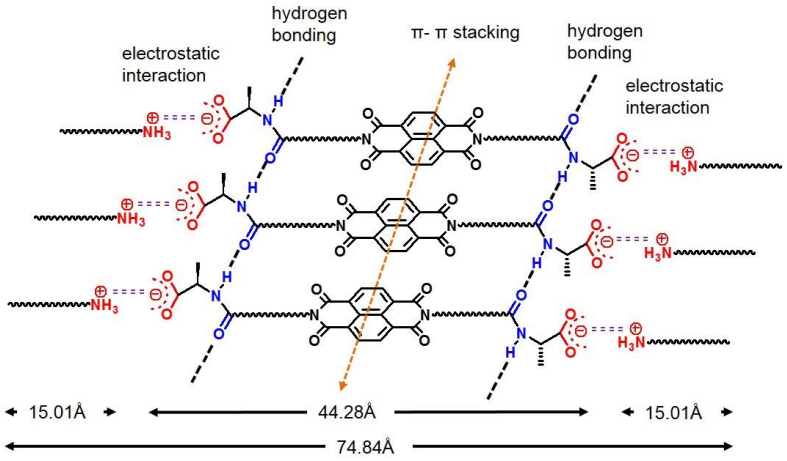

Figure 8. A tentative model for the molecular packing arrangements among the gelator molecules in the two-component co-assembled system obtained from FTIR, PXRD and SAXS data. The molecular length of dodecylamine (C12) has been used to calculate the total molecular length in the two-component co-assembled structure.

Fourier Transform Infrared (FT-IR) Analysis

In the solid state of peptide **P**, a characteristic peak due to C=O stretching frequency corresponding to the carboxylic acid (-COOH) was observed at 1707 cm^{-1}, whereas, in the xerogel state, the intensity of this peak is diminished (Figure 9). In the gel state, peaks due to the C=O stretch band of carboxylate anion appeared at 1584 cm^{-1} and 1392 cm^{-1} for **P10**. For **P12** hydrogel, these peaks are at 1582 cm^{-1} and 1408 cm^{-1}. This observation suggests that in the gel state, the gelator molecules are present in carboxylate ($-COO^-$) form. The presence of peaks corresponding to the N-H stretching frequency at 3307 cm^{-1} and 3308 cm^{-1}, and the amide carbonyl stretching frequency at 1640 cm^{-1} and 1646 cm^{-1} for **P10** and **P12** respectively indicate hydrogen bond formation in the gel state. The peaks at 3414 cm^{-1} and

3418 cm^{-1} can be assigned as the NH-stretching frequency of ammonium species of the amine part of two-component gels in their assembled state.

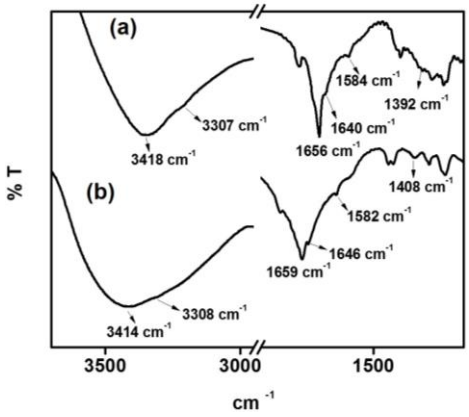

Figure 9. FT-IR spectra of the xerogels obtained from the hydrogels (a) **P10** and (b) **P12** (at a 1:2 molar ratio of peptide: amine).

Current-Voltage Study

Though there are several reports of semiconducting behavior of NDI-based soft-materials mainly obtained from organic solvents,[62] water processable NDI-based soft-material that shows semiconducting behavior is yet to be explored. Therefore, in this study the bulk electrical conductivity of peptide containing NDI-materials with corresponding amines in their co-assembled states have been measured by current-voltage study. It is evident from the I-V plot (Figure 10) that the increment of current with respect to the voltage applied follows a linear relationship in the low voltage region for both **P10** and **P12** xerogels (at 1:2 molar ratio of peptide: amine) in their respective co-assembled states, confirming the development of Ohmic contacts (V/I = R). However, in the higher voltage region, the I-V curves show deviation from the linearity. This indicates the semiconducting nature of these two-component systems. The conductivity of both **P10** and **P12** xerogels have been calculated to be 5.5-6 X 10^{-6} S cm^{-1}. These observations demonstrate an excellent electric semiconducting behavior for the two-component NDI-based systems in their xerogel states.

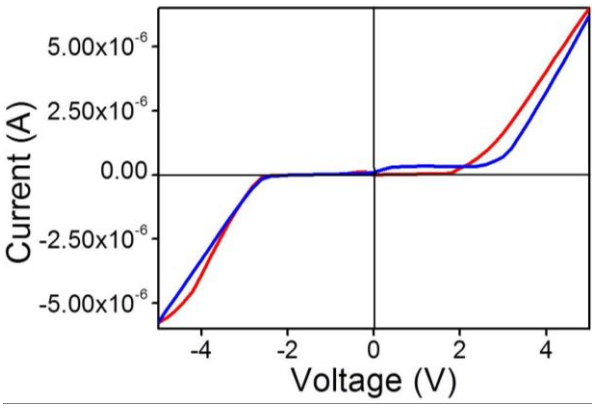

Figure 10. I-V characteristics shown by the two-component xerogels obtained from **P10** (blue line) and **P12** (red line) hydrogels at a 1:2 molar ratio of peptide: amine.

CONCLUSION

In summary, two-component fluorescent hydrogels have been made from peptide appended NDI moiety and long chain primary amines in aqueous medium. These gels have been thoroughly characterized by FTIR, XRD, SAXS, TEM and rheological experiments. Interestingly, thermal and mechanical strength of the gels has been nicely tuned by varying the alkyl chain length of the primary amines. Moreover, these two-component co-assembled gels exhibit appreciable semiconducting property as it is evident from their I-V characteristics. The discovery of NDI-based highly fluorescent two-component new soft materials in an eco-friendly solvent (water) opens up future directions for the development and construction of smart materials for applications in opto-electronic devices, fluorescence biosensors and other purposes.

ACKNOWLEDGEMENTS

N. N gratefully acknowledges CSIR, New Delhi, India for financial assistance. We acknowledge Rumana Parveen, Department of Organic Chemistry, IACS and Department of Bio-technology (DBT), New Delhi (DBT project number: BT/01/CEIB/11/V/13) for allow us to use Anton Paar modular compact rheometer (MCR 102) for rheological measurement.

ASSOCIATED CONTENT

Supporting Information

Experimental section, Instrumentation, Gel preparation, Synthetic procedures, NMR, MALDI-TOF MS, Spectroscopic study, SAXS and Rheological study. This information is available free of charge via the Internet at http://pubs.acs.org/.

REFERENCES

1. Caruso, M.; Gatto, E.; Placidi, E.; Ballano, G.; Formaggio, Toniolo, C.; Zanuy, D.; Alemánde, C.; Venanzi, M. A single-residue substitution inhibits fibrillization of Ala-based pentapeptides. A spectroscopic and molecular dynamics investigation. *Soft Matter* **2014**, *10*, 2508-2519.

2. Ziserman, L.; Lee, H. –Y.; Raghavan, S. R.; Mor, A.; Danino, D. Unraveling the Mechanism of Nanotube Formation by Chiral Self-Assembly of Amphiphiles. *J. Am. Chem. Soc.* **2011**, *133*, 2511-2517.

3. Oh, H.; Javvaji, V.; Yaraghi, N. A.; Abezgauz, L.; Danino, D.; Raghavan, S. R. Light-induced transformation of vesicles to micelles and vesicle-gels to sols. *Soft Matter* **2013**, *9*, 11576-11584.

4. Terech, P.; Dourdain, S.; Bhat, S.; Maitra, U. Self-Assembly of Bile Steroid Analogues: Molecules, Fibers, and Networks. *J. Phys. Chem. B* **2009**, *113*, 8252-8267.

5. Mallia, V. A.; Weiss, R. G. Correlations between thixotropic and structural properties of molecular gels with crystalline networks. *Soft Matter* **2016**, *12*, 3665-3676.

6. Feldner, T.; Häring, M.; Saha, S.; Esquena, J.; Banerjee, R.; Díaz, D. D. Supramolecular Metallogel That Imparts Self-Healing Properties to Other Gel Networks. *Chem. Mater*. **2016**, *28*, 3210-3217.

7. Armelin, E.; Pérez-Madrigal, M. M.; Alemán, C.; Díaz, D. D. Current status and challenges of biohydrogels for applications as supercapacitors and secondary batteries. *J. Mater. Chem. A* **2016**, *4*, 8952-8968.

8. Adler-Abramovich, L.; Gazit, E. The physical properties of supramolecular peptide assemblies: from building block association to technological applications. *Chem. Soc. Rev*. **2014**, *43*, 6881-6893.

9. Zhang, L.; Jin, Q.; Liu, M. Enantioselective Recognition by Chiral Supramolecular Gels. *Chem. Asian J*. **2016**, DOI: 10.1002/asia.201600441.

10. Maiti, D. K.; Banerjee, A. A Synthetic Amino Acid Residue Containing A New Oligopeptide-Based Photosensitive Fluorescent Organogel. *Chem. Asian J*. **2013**, *8*, 113-120.

11. Gupta, J. K.; Adams, D. J.; Berry, N. G. Will it gel? Successful computational prediction of peptide gelators using physicochemical properties and molecular fingerprints. *Chem. Sci*. **2016**, *7*, 4713-4719.

12. Singh, N.; Conte, M. P.; Ulijn, R. V.; Miravet, J. F.; Escuder, B. Insight into the esterase like activity demonstrated by an imidazole appended self-assembling hydrogelator. *Chem. Commun.* **2015**, *51*, 13213-13216.

13. Foster, J. A.; Edkins, R. M.; Cameron, G. J.; Colgin, N.; Fucke, K.; Ridgeway, S.; Crawford, A. G.; Marder, T. B.; Beeby, A.; Cobb, S. L.; Steed, J. W. Blending Gelators to Tune Gel Structure and Probe Anion-Induced Disassembly. *Chem. Eur. J*. **2014**, *20*, 279-291.

14. Cayuela, A.; Kennedy, S. R.; Soriano, M. L.; Jones, C. D.; Valcárcel, M.; Steed, J. W. Fluorescent carbon dot–molecular salt hydrogels. *Chem. Sci*. **2015**, *6*, 6139-6146.

15. Weiss, R. G. The Past, Present, and Future of Molecular Gels. What Is the Status of the Field, and Where Is It Going? *J. Am. Chem. Soc.* **2014**, *136*, 7519-7530.

16. Cardoso, A. Z.; Mears, L. L. E.; Cattoz, B. N.; Griffiths, P. C.; Schweins, R.; Adams, D. J. Linking micellar structures to hydrogelation for salt-triggered dipeptide gelators. *Soft Matter* **2016**, *12*, 3612-3621.

17. Baral, A.; Basak, S.; Basu, K.; Dehsorkhi, A.; Hamley, I. W.; Banerjee, A. Time-dependent gel to gel transformation of a peptide based supramolecular gelator. *Soft Matter* **2015**, *11*, 4944-4951.

18. Maity, M.; Sajisha, V. S.; Maitra, U. Hydrogelation of bile acid–peptide conjugates and in situ synthesis of silver and gold nanoparticles in the hydrogel matrix. *RSC Adv.* **2015**, *5*, 90712-90719.

19. Baral, A.; Roy, S.; Ghosh, S.; Merino, D. H.; Hamley, I. W.; Banerjee, A. A Peptide-Based Mechano-sensitive, Proteolytically Stable Hydrogel with Remarkable Antibacterial Properties. *Langmuir* **2016**, *32*, 1836-1845.

20. Zhou, J.; Du, X.; Gao, Y.; Shi, J.; Xu, B. Aromatic−Aromatic Interactions Enhance Interfiber Contacts for Enzymatic Formation of a Spontaneously Aligned Supramolecular Hydrogel. *J. Am. Chem. Soc*. **2014**, *136*, 2970-2973.

21. Yuan, D.; Du, X.; Shi, J.; Zhou, N.; Zhou, J.; Xu, B. Mixing Biomimetic Heterodimers of Nucleopeptides to Generate Biocompatible and Biostable Supramolecular Hydrogels. *Angew. Chem. Int. Ed.* **2015**, *54*, 5705-5708.

22. Jung, J. H.; Lee, J. H.; Silverman, J. R.; John, G. Coordination polymer gels with important environmental and biological applications. *Chem. Soc. Rev.* **2013**, *42*, 924-936.

23. Sun, J. E. P.; Stewart, B.; Litan, A.; Lee, S. J.; Schneider, J. P.; Langhans, S. A.; Pochan, D. J. Sustained release of active chemotherapeutics from injectable-solid β-hairpin peptide hydrogel. *Biomater. Sci.*, **2016**, *4*, 839-848.

24. Knerr, P. J.; Branco, M. C.; Nagarkar, R.; Pochan, D. J.; Schneider, J. P. Heavy metal ion hydrogelation of a self-assembling peptide via cysteinyl chelation. *J. Mater. Chem*. **2012**, *22*, 1352-1357.

25. Swanekamp, R. J.; Welch, J. J.; Nilsson, B. L. Proteolytic stability of amphipathic peptide hydrogels composed of self-assembled pleated β-sheet or coassembled rippled β-sheet fibrils. *Chem. Commun.* **2014**, *50*, 10133-10136.

26. da Silva, E. R.; Walter, M. N. M.; Reza, M.; Castelletto, V.; Ruokolainen, J.; Connon, C. J.; Alves, W. A.; Hamley, I. W. Self-Assembled Arginine-Capped Peptide Bolaamphiphile Nanosheets for Cell Culture and Controlled Wettability Surfaces. *Biomacromolecules* **2015**, *16*, 3180-3190.

27. Liu, Y.; Chen, C.; Wang, T.; Liu, M. Supramolecular Chirality of the Two-Component Supramolecular Copolymer Gels: Who Determines the Handedness? *Langmuir* **2016**, *32*, 322-328.

28. Hirst, A. R.; Smith, D. K.; Feiters, M. C.; Geurts, H. P. M. Two-Component Dendritic Gel: Effect of Spacer Chain Length on the Supramolecular Chiral Assembly. *Langmuir* **2004**, *20*, 7070-7077.

29. Hirst, A. R.; Miravet, J. F.; Escuder, B.; Noirez, L.; Castelletto, V.; Hamley, I. W.; Smith, D. K. Self-Assembly of Two-Component Gels: Stoichiometric Control and Component Selection. *Chem. Eur. J.* **2009**, *15*, 372-379.

30. Hu, Z.; Pantoş, G. D.; Kuganathan, N.; Arrowsmith, R. L.; Jacobs, R. M. J.; Kociok-Köhn, G.; O'Byrne, J.; Jurkschat, K.; Burgos, P.; Tyrrell, R. M.; Botchway, S. W.; Sanders, J. K. M.; Pascu, S. I. Interactions Between Amino Acid-Tagged Naphthalenediimide and Single Walled Carbon Nanotubes for the Design and Construction of New Bioimaging Probes. *Adv. Funct. Mater*. **2012**, *22*, 503-518.

31. Ryan, S. T. J.; Young, R. M.; Henkelis, J. J.; Hafezi, N.; Vermeulen, N. A.; Hennig, A.; Dale, E. J.; Wu, Y.; Krzyaniak, M. D.; Fox, A.; Nau, W. M.; Wasielewski, M. R.; Stoddart, J. F.; Scherman, O. A. Energy and Electron Transfer Dynamics within a Series of Perylene Diimide/Cyclophane Systems. *J. Am. Chem. Soc*. **2015**, *137*, 15299-15307.

32. Hou1, X.; Ke1, C.; Bruns, C. J.; McGonigal, P. R.; Pettman, R. B.; Stoddart, J. F. Tunable solid-state fluorescent materials for supramolecular encryption. *Nat. Comm.* **2015**, (1-6).

33. Yuan, Z.; Ma, Y.; Geßner, T.; Li, M.; Chen, L.; Eustachi, M.; Weitz, R. T.; Li, C.; Müllen, K. Core-Fluorinated Naphthalene Diimides: Synthesis, Characterization, and Application in n‐Type Organic Field-Effect Transistors. *Org. Lett.* **2016**, *18*, 456-459.

34. Pandeeswar, M.; Govindaraju, T. Engineering molecular self-assembly of perylene diimide through pH-responsive chiroptical switching. *Mol. Syst. Des. Eng*. **2016**, DOI: 10.1039/c6me00012f.

35. Babu, S. S.; Praveen, V. K.; Ajayaghosh, A. Functional π‐Gelators and Their Applications. *Chem. Rev*. **2014**, *114*, 1973-2129.

36. Yun, S. W.; Kim, J. H.; Shin, S.; Yang, H.; An, B. -K.; Yang, L.; Park, S. Y. High-Performance n-type Organic Semiconductors: Incorporating Specific Electron-Withdrawing Motifs to Achieve Tight Molecular Stacking and Optimized Energy Levels. *Adv. Mater.* **2012**, *24*, 911-915.

37. Aparicio, F.; Cherumukkil, S.; Ajayaghosh, A.; Sánchez, L. Color-Tunable Cyano-Substituted Divinylene Arene Luminogens as Fluorescent π-Gelators. *Langmuir* **2016**, *32*, 284-289.

38. Das, J.; Siram, R. B. K.; Cahen, D.; Rybtchinski, B.; Hodes, G. Thiophene-modified perylenediimide as hole transporting material in hybrid lead bromide perovskite solar cells. *J. Mater. Chem. A* **2015**, *3*, 20305-20312.

39. Anderson, T. W.; Pantoş, G. D.; Sanders, J. K. M. Supramolecular chemistry of monochiral naphthalenediimides. *Org. Biomol. Chem.* **2011**, *9*, 7547-7553.

40. Zhao, Y.; Cotelle, Y.; Sakai, N.; Matile, S. Unorthodox Interactions at Work. *J. Am. Chem. Soc.* **2016**, *138*, 4270-4277.

41. Suraru, S. -L.; Würthner, F. Strategies for the Synthesis of Functional Naphthalene Diimides. *Angew. Chem. Int. Ed.* **2014**, *53*, 7428-7448.

42. Wang, S.; Pisula, W.; Müllen, K. Nanofiber growth and alignment in solution processed n-type naphthalene-diimide-based polymeric field-effect transistors. *J. Mater. Chem.* **2012**, 22, 24827-24831.

43. Shao, H.; Nguyen, T.; Romano, N. C.; Modarelli, D. A.; Parquette, J. R. Self-Assembly of 1-D n-Type Nanostructures Based on Naphthalene Diimide-Appended Dipeptides. *J. Am. Chem. Soc.* **2009**, *131*, 16374-16376.

44. Basak, S.; Nanda, J.; Banerjee, A. Assembly of naphthalenediimide conjugated peptides: aggregation induced changes in fluorescence. *Chem. Commun.* **2013**, *49*, 6891-6893.

45. Basak, S.; Nandi, N.; Bhattacharyya, K.; Datta, A.; Banerjee, A. Fluorescence from an H-aggregated naphthalenediimide based peptide: photophysical and computational investigation of this rare phenomenon. *Phys. Chem. Chem. Phys*. **2015**, *17*, 30398-30403.

46. Bhosale, S. V.; Jani, C. H.; Langford, S. J. Chemistry of naphthalene diimides. *Chem. Soc. Rev*. **2008**, *37*, 331-342.

47. Peebles, C.; Wight, C. D.; Iverson, B. L. Solution- and solid-state photophysical and stimuli-responsive behavior in conjugated monoalkoxynaphthalene–naphthalimide donor–acceptor dyads. *J. Mater. Chem. C* **2015**, *3*, 12156-12163.

48. Kulkarni, C.; George, S. J. Carbonate Linkage Bearing Naphthalenediimides: Self-Assembly and Photophysical Properties. *Chem. Eur. J*. **2014**, 20, 4537-4541.

49. Hong, Y.; Lama, J. W. Y.; Tang, B. Z. Aggregation-induced emission. *Chem. Soc. Rev*. **2011**, *40*, 5361-5388.

50. Basak, S.; Nandi, N.; Baral, A.; Banerjee, A. Tailor-made design of J- or H-aggregated naphthalenediimide-based gels and remarkable fluorescence turn on/off behaviour depending on solvents. *Chem. Commun.* **2015**, *51*, 780-783.

51. Sakai, N.; Mareda, J.; Vauthey, E.; Matile, S. Core-substituted naphthalenediimides. *Chem. Commun.* **2010**, *46*, 4225-4227.

52. Görl, D.; Zhang, X.; Würthner, F. Molecular Assemblies of Perylene Bisimide Dyes in Water. *Angew. Chem. Int. Ed.* **2012**, *51*, 6328-6348.

53. Nalluri, S. K. M.; Berdugo, C.; Javid, N.; Frederix, P. W. J. M.; Ulijn, R. V. Biocatalytic Self-Assembly of Supramolecular Charge-Transfer Nanostructures Based on n-Type Semiconductor-Appended Peptides. *Angew. Chem. Int. Ed.* **2014**, *53*, 5882-5887.

54. Nandre, K. P.; Bhosale, S. V.; Krishna, K. V. S. R.; Gupta, A.; Bhosale, Sidhanath V. A phosphonic acid appended naphthalene diimide motif for self-assembly into tunable nanostructures through molecular recognition with arginine in water. *Chem. Commun.* **2013**, *49*, 5444-5446.

55. Shao, H.; Seifert, J.; Romano, N. C.; Gao, M.; Helmus, J. J.; Jaroniec, C. P.; Modarelli, D. A.; Parquette, J. R. Amphiphilic Self-Assembly of an n-Type Nanotube. *Angew. Chem. Int. Ed.* **2010**, *49*, 7688-7691.

56. Shao, H.; Gao, M.; Kim, S. H.; Jaroniec, C. P.; Parquette, J. R. Aqueous Self-Assembly of l-Lysine-Based Amphiphiles into 1D n-Type Nanotubes. *Chem. Eur. J.* **2011**, *17*, 12882-12885.

57. Shao, H.; Parquette, J. R. A π-conjugated hydrogel based on an Fmoc-dipeptide naphthalenediimide semiconductor. *Chem. Commun.* **2010**, *46*, 4285-4287.

58. Zhan, F. -K.; Hsu, S. -M.; Cheng, H.; Lin, H. -C. Remarkable influence of alkyl chain lengths on supramolecular hydrogelation of naphthalene diimide-capped dipeptides. *RSC Adv.* **2015**, *5*, 48961-48964.

59. Liu, Y. –H.; Hsu, S. –M.; Wu, F. –Y.; Cheng, H.; Yeh, M. –Y.; Lin, H. -C. Electroactive Organic Dye Incorporating Dipeptides in the Formation of Self-Assembled Nanofibrous Hydrogels. *Bioconjugate Chem.* **2014**, *25*, 1794-1800.

60. Hsu, L. -H.; Hsu, S. -M.; Wu, F. -Y.; Liu, Y. -H.; Nelli, S. R.; Yeh, M. -Y.; Lin, H. -C. Nanofibrous hydrogels self-assembled from naphthalene diimide (NDI)/amino acid conjugates. *RSC Adv.* **2015**, *5*, 20410-20413.

61. Basu, K.; Baral, A.; Basak, S.; Dehsorkhi, A.; Nanda, J.; Bhunia, D.; Ghosh, S.; Castelletto, V.; Hamley, I. W.; Banerjee, A. Peptide based hydrogels for cancer drug release: modulation of stiffness, drug release and proteolytic stability of hydrogels by incorporating D-amino acid residue(s). *Chem. Commun.* **2016**, *52*, 5045-5048.

62. Jain, A.; George, S. J. New directions in supramolecular electronics. *Mater. Today* **2015**, *18*, 206-214.

Table of Contents (TOC)